Journal of Biomedical Optics

BiomedicalOptics.SPIEDigitalLibrary.org

Review of the progress toward achieving heat confinement—the holy grail of photothermal therapy

Wangzhong Sheng
Sha He
William J. Seare
Adah Almutairi

SPIE.

Wangzhong Sheng, Sha He, William J. Seare, Adah Almutairi, "Review of the progress toward achieving heat confinement—the holy grail of photothermal therapy," *J. Biomed. Opt.* **22**(8), 080901 (2017), doi: 10.1117/1.JBO.22.8.080901.

Journal of Biomedical Optics 22(8), 080901 (August 2017)

REVIEW

Review of the progress toward achieving heat confinement—the holy grail of photothermal therapy

Wangzhong Sheng,[a,b] Sha He,[b,c] William J. Seare,[d] and Adah Almutairi[a,b,c,*]
[a]University of California, Laboratory for Bioresponsive Materials, Department of Mechanical and Aerospace Engineering, Materials Science Program, La Jolla, San Diego, California, United States
[b]University of California, Laboratory for Bioresponsive Materials, Skaggs School of Pharmacy and Pharmaceutical Sciences, La Jolla, San Diego, California, United States
[c]University of California, Laboratory for Bioresponsive Materials, Department of Nanoengineering, La Jolla, San Diego, California, United States
[d]Clinique Sculpture, Carlsbad, California, United States

Abstract. Photothermal therapy (PTT) involves the application of normally benign light wavelengths in combination with efficient photothermal (PT) agents that convert the absorbed light to heat to ablate selected cancers. The major challenge in PTT is the ability to confine heating and thus direct cellular death to precisely where PT agents are located. The dominant strategy in the field has been to create large libraries of PT agents with increased absorption capabilities and to enhance their delivery and accumulation to achieve sufficiently high concentrations in the tissue targets of interest. While the challenge of material confinement is important for achieving "heat and lethality confinement," this review article suggests another key prospective strategy to make this goal a reality. In this approach, equal emphasis is placed on selecting parameters of light exposure, including wavelength, duration, power density, and total power supplied, based on the intrinsic properties and geometry of tissue targets that influence heat dissipation, to truly achieve heat confinement. This review highlights significant milestones researchers have achieved, as well as examples that suggest future research directions, in this promising technique, as it becomes more relevant in clinical cancer therapy and other noncancer applications. [DOI: 10.1117/1.JBO.22.8.080901]

Keywords: photothermal therapy; selective photothermolysis; nanomedicine; gold nanoparticles.

Paper 170036VR received Jan. 30, 2017; accepted for publication Jun. 23, 2017; published online Aug. 4, 2017.

1 Introduction

Cancer, characterized by uncontrolled cellular growth, is one of the leading causes of death in the United States.[1] Nearly 1.7 million newly diagnosed cases of cancer were reported in 2015, of which about 35% of affected patients died from the disease.[2] Since cancer incidence rates track closely with our growing aging population, these numbers are expected to continue to increase in the future. Cancer is not just one disease; it is extremely complex and can be found in many forms. Through continuous and enormous effort, we have gained a better understanding of cancer, although there is still much we do not know. What is clear is that cancer treatments almost universally require a multipronged approach to improve overall disease prognosis.[3–5] Currently, the primary prong of cancer therapy is surgery, which is often complemented by the subprongs of chemo[6] and radiation therapy[7] to bolster effectiveness. Nevertheless, resistance to treatment often leads to cancer recurrence, especially in the cases of certain malignant cancers.[8] Additionally, the highly invasive nature, limited indication and success, substantial cost, and pain of surgery, as well as potential complications with expected and unexpected side-effects of adjuvant therapies, all lead to reduced quality of life and reduced life expectancy for surviving patients.[9–11] Photothermal therapy (PTT) has recently emerged as a potential area of promise for this multipronged approach to cancer therapy.[12–16] In PTT, the core concept is to apply otherwise benign near-infrared (NIR) light that can reach several centimeters beneath the skin surface[17] in combination with highly efficient photothermal (PT) agents placed noninvasively within tissues to create hypothermia to damage cancers only where the agents are placed, offering unprecedented safety, specificity, and selectivity in eradicating cancer.

Historically, hyperthermia through heating has proven to be extremely effective in inducing damage, especially to biological tissues.[18] In general, there is a time–temperature-dependent relationship such that the higher the temperature, the more rapidly the tissues become damaged, with the likelihood of damage exponentially doubling above 43°C.[19] In tumors, the capacity for heat dissipation is significantly reduced due to the tortuous blood vessel network the cancers form, making them even more susceptible to thermal treatments.[20] Despite this difference, care must be taken to precisely define where the heating occurs so that the surrounding healthy tissue is not accidentally damaged in the heating process. This concept is called heat confinement and is often not achievable with traditional heating methods.[21] Light-induced heating with the aid of PT agents has the advantage of affording more control over where the selected tissue heating occurs. However, the general drawback of poor tissue penetration-depth in light-based biological applications still must be overcome. Thus, the overall problem of selectively delivering heat to, and confining it within tissues, is one of the major challenges of PTT.

In order to achieve light-induced heat confinement, highly efficient PT agents must first be sequestered inside the tumor

*Address all correspondence to: Adah Almutairi, E-mail: aalmutairi@ucsd.edu

1083-3668/2017/$25.00 © 2017 SPIE

at sufficient concentrations to absorb the deep-penetrating NIR light. Early incarnations of PTT involved the direct injection of concentrated mixtures of PT agents into tumor xenografts followed by continuous and long-term exposure to high-powered lasers.[13,15,22] These initial outcomes often caused nonselective and uncontrolled heating to extreme temperatures, not unlike that of direct heating methods. These treatments resulted in immediate cellular death of both cancerous and noncancerous tissues in the exposed regions. The mechanism of damage was that of well-known tissue hyperthermia, dominated by necrosis accompanied by irreparable denaturation of proteins and other biological macromolecules.[23] While some of these proof-of-concept models demonstrated the ability of PTT to reduce tumor volume or prolong the survival of treated animals,[24] clinically, they are generally not feasible or practical. Additionally, as is usually the case with introducing any foreign substance into biological systems, it is also important to mitigate any potential toxicity associated with these exogenous agents.[25,26] This will be no easy feat and will likely require careful consideration of the multifactorial interactions between diverse and complex disease states found in cancer biology with the various engineered nanomedicine platforms delivering the cancer therapies. Thus, the delivery of PTT agents to the desired targets of interest is a second major challenge.

This review focuses on the current state of development of this promising technology over many years, its recent advances, as well as obstacles that must still be overcome (Fig. 1). We begin by introducing the theory behind the PT conversion process and examining examples where the PT effect was successfully applied toward heating of naturally existing pigments. In this context, the principle of selective photothermolysis (SPT) is presented, where specific parameters of light exposure are chosen based on the size and geometry of biological targets of interest to achieve heat confinement in pigmented tissues. We propose this principle as a strategy to potentially achieve more selective light-induced heat confinement in PTT. Some of the leading, highly efficient, man-made PT agents that enable this technique are then summarized, although we opted to take a succinct approach due to the vast amount of research published on this topic. We also briefly comment on the potential sources of toxicity of popular PT agents as well as strategies that have been employed to address these concerns. In Sec. 4, we expand on the topic of drug delivery and provide an overview of cases, in which the PT effect was leveraged synergistically with diagnostic or other therapeutic agents, to garner theranostic or multimodal therapeutic nanomedicine platforms, respectively, for cancer therapy. Finally, we speculate on critical avenues for further research and development that could make this technique more clinically relevant.

2 Light Tissue Interactions

The interaction of light with matter is extremely complex.[27–31] In general, when light impinges on matter, it interacts with the electromagnetic field of the atoms in the material and as a result, many complex phenomena occur. The interaction depends on important factors such as the wavelength and power density of light, but just as importantly, it depends on the properties of the interacting species itself. Different species can reflect, diffract, polarize, absorb, and disperse light. Additionally, many complex nonlinear optical effects may occur.[30] Nevertheless, in describing the PT effect, especially in diffuse anisotropic media such as biological tissue, many of these observed phenomena can be categorized as absorption or scattering.[32,33] Simplistically, absorption describes the amount of incident energy that is captured, whereas scattering describes any energy that is not.[33–35] Absorption can be further distinguished into absorption by the target species or by unwanted species. Light that is competitively absorbed or scattered is said to be attenuated or reduced in intensity. Additionally, depending on the PT absorber, not all of the electromagnetic energy may be converted to heat. For example, instead it could be used to drive chemical reactions in applications such as photodynamic therapy (PDT).[36,37] Absorbed light may also be re-emitted as another wavelength of light, e.g., fluorescence.[38,39] Good PT agents will not only capture a large percentage of the incident light, but also effectively transform it into heat, and are said to have high PT conversion efficiencies.[40–42] The most commonly used model to describe absorption is the Beer–Lambert law[43]

$$A_\lambda = \varepsilon c l,$$

where A_λ is the absorption [optical density (OD)] of the material at wavelength λ, ε is the molar extinction coefficient, c is the molar concentration, and l is the path length that the light travels through the absorbing medium. The Beer–Lambert law is quite accurate in describing light-matter phenomenon in cuvette settings,[44] although actual observed behavior starts to deviate from this law if any major assumptions are not met. Unfortunately, biological tissue is one such medium. It contains several non-independently absorbing pigmented species that may competitively absorb incident light in the highly inhomogeneous and turbid tissue environment.[45,46] Therefore, the expected trends defined by this equation should serve only as a general reference when assessing absorbers for PT applications.

2.1 *Biological Optical Window*

One of the biggest limitations in light-based biological applications is penetration depth.[47–49] The strongest naturally existing species contributing to light attenuation by surface tissues are melanin, hemoglobin, and water.[50] Melanin is a pigmented protein produced by melanocytes concentrated in the basal layer of the epidermis. Melanin has a local absorption maximum around 350 nm that decreases gradually progressing into the visible wavelengths of the electromagnetic spectra and beyond.[51] As a result, longer wavelengths of light can penetrate deeper into tissues. The amount of melanin in skin varies across different populations of people and increases with sun exposure.[52] Melanin content in skin is typically classified by the Fitzpatrick scale of skin colors, with level I being very pale through level VI being very dark.[53,54] In all skin types, some of the penetrating light energy is absorbed by melanin. In darker skin types, melanin is present in significantly higher concentrations so even longer light wavelengths will have difficulty penetrating beyond the epidermis.[43,44]

Like melanin, hemoglobin also exhibits large absorptions at longer wavelengths, with a sharp drop at ~600 nm for both the oxygenated and deoxygenated forms.[55] Dragan and Geddes[56] measured the absorption of whole human blood sandwiched between two glass slides and found that at 800 nm, the absorption of a 1-mm-thick sample, which could be representative of a small blood vessel, was 0.5 OD. Described in terms of the Beer–Lambert law, this OD means that nearly 70% of incident light is absorbed. Fortunately, hemoglobin's contribution to light attenuation is more variable than melanin's, since its absorption

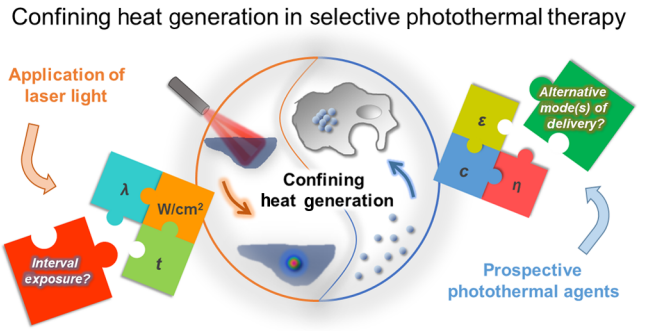

Fig. 1 Schematic highlighting factors crucial to achieving material and heat confinement in PTT; current research directions involve alternative parameters of light exposure to modulate tissue heating, or alternative methods of delivery, such as intravenous or local sustained-delivery, as opposed to bolus IT injections that are typically considered the norm in PTT. Abbreviations: (application of laser light) λ, wavelength; W/cm^2, power density; t, exposure time; (prospective photothermal agents) ε, extinction coefficient; c, concentration; and η, PT conversion efficiency.

is dictated by the size and number of blood vessels, which, generally, are distributed nonhomogenously in any given tissue. Thus, it appears that longer wavelengths of light beyond 600 nm would be preferred for transcutaneous biological applications.

However, there exists an upper limit of around 1000 nm, where another strongly absorbing "pigment," water[57] can significantly limit light penetration into tissue. Since human epidermis is on average 64.6% water,[58,59] in addition to being the primary harbinger of melanin, it is the largest barrier of entry for light in the infrared regime of the EM spectrum. Because of this, techniques that have shown promise in achieving heat confinement, such as laser interstitial thermal therapy, a minimally invasive, contrast-agent-free, laser PT technique that relies on absorption of water-resonant wavelengths of light by the water molecules in tissue to directly ablate benign and malignant lesions, requires the percutaneous insertion of a fiber-optic catheter directly into tissues to bypass the skin barrier to achieve therapeutic efficacy.[60] It would be desirable to be able to use wavelengths of light that can more readily bypass the optical skin barrier. Incidentally, when the absorption profiles of melanin, hemoglobin, and water are overlaid, a region of minimal absorption between 600 and 1000 nm emerges. This range of wavelengths is commonly referred to as the biological optical window (Fig. 2).[61,62] Light in the middle of this near-infrared (NIR) region (around 800 nm) can penetrate through skin and up to several centimeters into tissue,[17] making NIR absorbing species especially attractive for transcutaneous PT applications.[39,63]

2.2 *Selective Photothermolysis to Overcome Attenuation by Endogenous Species*

Although endogenous species are responsible for the limited penetration depth of light, they have also been successful targets

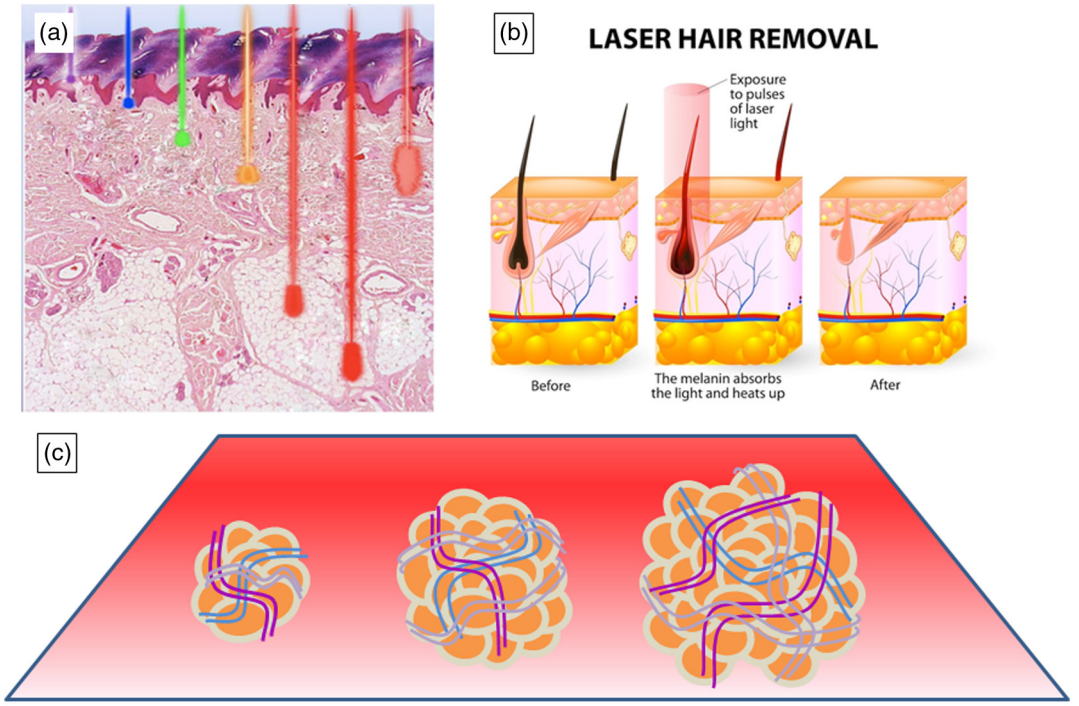

Diameter	1 cm	2 cm	3 cm
T_R	30 sec	2 min	5 min

Fig. 2 (a) Wavelengths between 700 and 900 nm are minimally absorbed by endogenous species and are able to penetrate deepest into tissue.[49] Reproduced from Ref. 49. © 2013. (b) Schematic demonstrating underlying principles behind laser hair removal technologies. Reproduced from Dr. Gayne Dolyan Descornet, "How does laser hair removal work," Woman Health and Life. (c) Thermal relaxation times (T_R) for spherical structures, e.g., tumors, of various sizes, according to SPT theory. Treatment times in PTT are typically well above this regime.

of PT applications in the tangential field of cosmetics. PT targeting of melanin, in the form of laser hair removal,[64,65] and PT targeting of hemoglobin, in the treatment of port-wine stains[66] and varicose veins,[67,68] and have been widely and successfully applied in the clinic for decades. These applications take advantage of the fact that in biological structures such as hair follicles and blood vessels, there is a locally higher concentration of melanin and hemoglobin, respectively, than is present within surrounding tissues. If the targeted structure absorbs the defined wavelength at least twice as much as its immediate surroundings, it is possible to selectively heat the target structure to damage it by optimizing the way in which light energy is applied to achieve heat confinement. Cooling of the skin surface can help to counteract some of the heating of the melanin, especially in darker skin types, to allow for the preservation of the sensitive dividing epidermal cells in the basal skin layer, while the deeper hair shafts are heated much more, relatively. In general, for transcutaneous applications, the higher the difference in absorption between the target structures and the surrounding tissues, including the skin, the easier it is to achieve heat confinement. This process, first proposed by Anderson,[69,70] is known as SPT.

In SPT, light is applied in a controlled pulsatile manner over a large region. Here, the strongly absorbing target structure will heat up much more than surrounding less-absorbing structures. The time it takes for the target structure to exponentially decay from the maximum temperature reached is described by the thermal relaxation time τ_R, which is dictated primarily by the size, geometry, and local density of the target structures. A core concept in SPT is to apply short, repeated bursts of light energy absorbed preferentially by the target structures before heat can dissipate or diffuse to adjacent tissues (relaxation), resulting in the continual build-up of heat, thereby creating a selective-heating effect. The overall exposure time should be less than the thermal relaxation time of the target structure to ensure that the surrounding areas experience only mild temperature elevations. Another caveat is that pulses must not be too short in order to avoid any cavitation effects which may be induced by the high powers achieved as a result of the short pulses.[71]

Heat transfer within tissues is governed by intrinsic properties of tissue such as thermal diffusivity, which is on the order of 10^{-3} cm^2/s. Approximating this term to be the same for both the target and its surroundings, Anderson and Parrish[69] calculated the τ_R for spherical targets with a wide range of sizes. For example, a spherical structure 1 mm in diameter has a τ_R of 0.3 s. By taking into consideration other intrinsic properties of tissue such as density and specific heat, appropriate powers and durations of light exposure could be calculated for SPT of target structures of various shapes and sizes (Fig. 2).[70] Altshuler et al. later expanded on this theory and proposed that due to the inexactness of the estimates, in practice, a buffer zone slightly larger than the absorbing structure should be defined with a threshold temperature set at this boundary that should not be exceeded. These engineering principles formed the foundation and continued to serve as the guiding principles for the development of laser-based cosmetic technologies.[72]

Although SPT applied toward endogenous species does not overcome the problem of penetration depth, the unique ability to confine heat to specific targetable pigmented structures, while sparing the surrounding tissue, could prove extremely powerful in the context of practical PTT. In the case of PT heating of exogenous species, the major advantage, and challenge, is that one could create an absorbing structure by virtue of where the PT absorber is introduced. If we examine the optical aspects and apply the principles of SPT theory toward PTT, we find that in the majority of demonstrations of PTT, heating is rarely confined. Researchers typically continuously expose target regions to high laser powers, resulting in uncontrolled damage leading to necrosis of the treated region and beyond.[73] Instead, we might propose that the thermal relaxation time could be estimated for different sized target tumors or metastases to determine the optimum parameters that should be used to limit the extent of PT heating and improve the specificity of PTT. Extending Anderson's calculations further, spherical structures 2 and 3 cm in diameter would have τ_R of ~2 and 5 min, respectively (Fig. 2). SPT for structures of any larger sizes may not be as applicable since rarely do tumors studied in a research setting exceed this size, and tumors of this size are likely to be resected clinically.[74] We have found examples in the literature where researchers have carefully considered how light is best applied based on the geometry of the target structures in order to maximize the specificity of the light-based application.[5,16,72,75,76] Furthermore, our own research lab is attempting to leverage this phenomenon in the context of liposuction to modulate heating of adipose tissues to aid in their removal by plastic surgeons.[72]

3 Photothermal Materials Platforms

Ultimately, the SPT of tumors is enabled by the large differential light absorption between the target and the surrounding tissues. To that end, in this section, we briefly summarize some of the leading man-made PT agents that have been applied for PTT.

3.1 *Exogenous Agents for Photothermal Therapy*

Many candidates have been explored for the PT killing of cancer both *in vitro* and *in vivo* (Fig. 3), with varying degrees of success. Arguably, the most widely applied class of PT agents is gold-based nanostructures, whose synthesis, characterization, standardization, and diverse properties have been extensively studied.[77–83] The mechanism of light-to-heat conversion is a localized form of surface plasmon resonance (LSPR).[84] This process is extremely efficient, and as a result, these materials exhibit one of the highest extinction coefficients reported,[85,86] on the order of 10^9 M^{-1} cm^{-1}. Since the absorbing LSPR peak and PT conversion efficiency are strongly dependent upon the geometry of the nanostructure,[87] researchers have engineered gold nanoparticles of many shapes and sizes to absorb preferentially within the biological window regime for PTT.

The simplest of all the geometries is probably the solid gold spherical nanoparticle. Around the early 2000s, the El-Sayed group synthesized and studied the plasmonic properties of solid gold nanospheres and found that although they were able to control the particle's LSPR peak by tuning its size, the peak was still less than 600 nm,[88] making it not practical as a candidate for PTT. To overcome this limitation, the group investigated the plasmonic properties of gold nanorods (AuNRs) and found that the anisotropic geometry of these nanostructures resulted in the establishment of a second LSPR peak corresponding to the longitudinal direction of the elongated rod-like structure.[12] Simulations suggested that by varying the aspect ratio of the nanorods, the LSPR peak could be precisely tuned to absorb a wide range of wavelengths in the NIR regime.[89] It took several years for a reproducible technique to synthesize AuNRs to be developed,[90] and several more years before AuNRs were applied for PTT in an *in vivo* setting.[13] In this study, Dickerson et al.

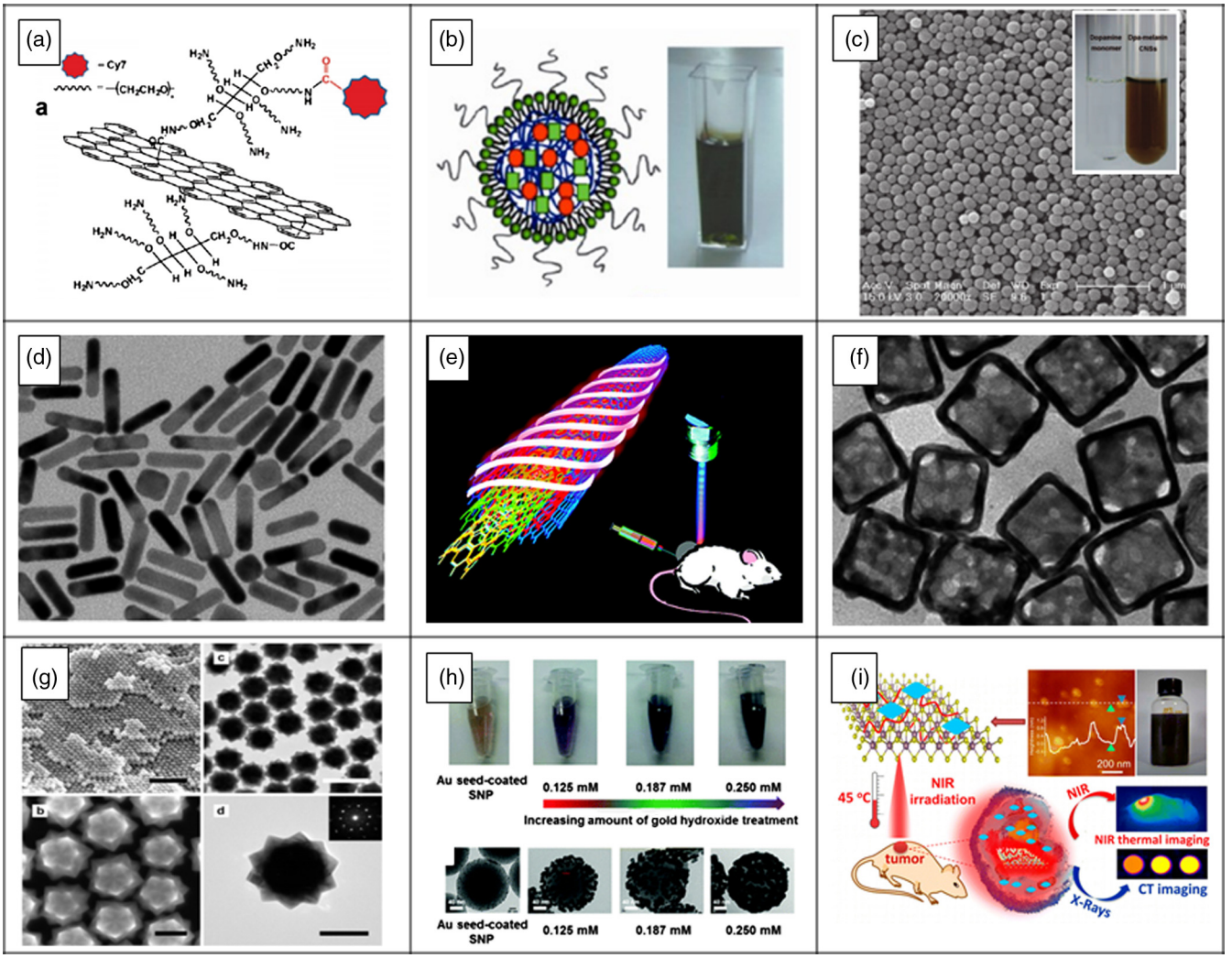

Fig. 3 Examples of photosensitizers applied for PTT: (a) graphene,[109] (b) indocyanine green-loaded polymer nanoparticles,[169] (c) melanin-HSA nanoparticles,[129] (d) gold nanorods,[101] (e) multiwalled carbon nanotubes,[76] (f) gold nanocages,[101] (g) gold nanostars,[100] (h) gold nanoshells,[93] and (i) MoS_2 nanoplates.[183] (a), (b), (d), (e), (f), and (i) are reprinted with permission from the American Chemical Society, © 2010, 2013, 2013, 2009, 2013, 2014, respectively. (c) is reprinted from permission from John Wiley & Sons, Inc. © 2013. (g) is not subject to U.S. copyright. (h) is reprinted with permission from The Royal Society of Chemistry. © 2015.

demonstrated the ability of plasmonic PTT to treat cancer in a squamous cell carcinoma xenograft model. The authors injected AuNRs either intratumorally (IT; 15 μL, $OD_{\lambda=800} = 40$) or intravenously (IV; 100 μL, $OD_{\lambda=800} = 120$) followed by 10 min of laser exposure and compared the outcome to a negative saline control. Both procedures outperformed the control with the authors observing a >57% tumor resorption for the IT-injected group versus 25% for the IV-injected group. However, the IV injected group, which likely relied on passive accumulation via the enhanced permeation and retention (EPR) effect[91] for delivery, required 20 times more AuNRs in combination with a laser power density almost double that of the intratumorally injected group, yet resulted in less tumor destruction (25% versus 57%, respectively).[13] This is not surprising, given that a recent analysis of the literature found that in less than 1% of the time did injected nanoparticles successfully penetrate solid tumors.[92]

Around the same time, the Halas and West groups utilized a slightly different approach to engineer gold nanoparticles which could absorb in the NIR regime in the form of gold nanoshells (AuNSs). AuNS are created by depositing a thin layer of gold on a dielectric nanoparticle substrate, most commonly, silica.[93,94] Similar to nanorods, the LSPR peak of nanoshells could be controlled by tuning the thickness of the shell, with the absorption maxima of thinner shells more red-shifted than thicker shells.[95] Hirsch et al.[15] applied these 100-nm gold–silica nanoshells in an *in vitro* and *in vivo* setting for plasmonic PTT. In the *in vitro* study, the authors incubated human breast epithelial carcinoma cells in a serum-free medium containing 4.4×10^9 PEGylated nanoshells per milliliter. After 1 h, nanoshells were rinsed away and a coherent NIR light source at 820 nm, 35 W/cm^2 was used to irradiate the cells for 7 min to induce PT damage. Compared to the area treated with the laser in the absence of nanoshells, the photothermally treated regions saw significantly more cell death. For the *in vivo* demonstration of PTT, 20 to 50 μL of gold–silica nanoshells were intratumorally injected 5 mm into the tumor volume and subsequently exposed to 820 nm light at 4 W/cm^2 at a 5-mm spot diameter for up to

6 min. The authors observed temperature elevations of 37.4°C ± 6.6°C within 4 to 6 min of light exposure which induced irreversible damage to the tumor. However, examination of the thermal profiles as a function of depth revealed that the maximum temperature elevation was found at just 1 mm below the skin surface, even though the nanoshells were injected 5 mm deep into the tumor.[15] It is likely that the AuNSs were distributed throughout the injection site, so PT ablation of the surface tissues with the high powers applied may have created a carbonaceous layer which would have exacerbated light attenuation as the PT treatment proceeded.[22]

Many more PT agents with large effective absorptions have been developed, albeit they faced many of the same challenges described above. In terms of plasmonic PT agents, additional nanostructures with exotic geometries have been synthesized and studied, including gold nanocubes, nanotetrahedron, and nanoicosahedrons,[96] nanocages,[97] nanostars,[44,98–100] and nanohexatripods.[101] Nongold-based plasmonic nanostructures such as quantum dots,[102] porous palladium nanoparticles,[103] and silver nanoparticles[104] have also been developed for plasmonic PTT. In addition to plasmonic PT nanomaterials, carbon-based agents such as single-walled[105] and multiwalled[76,106] carbon nanotubes,[107] and graphene sheets,[108–111] which rely on the vibration of excited, delocalized sp^2 electrons in the lattice of the carbon structure for heat generation,[76] have also been developed. Various small-molecule organic dyes absorbing in the NIR window such as indocyanine green (ICG),[22] cypate,[112,113] and porphyrins,[114,115] have also been applied for PTT. In the case of these agents, various engineered nanostructures, such as micelles[14,116–121] and biopolymer-based nanoparticles,[38,122,123] need to be employed to prolong the residence time of the agents to make them applicable for PTT, because they are prone to photobleaching[124] and are rapidly cleared from the body.[125] Sometimes, the polymer particles themselves can be applied directly as PT agents, as is the case with the conducting polymer, polypyrrole.[84,126,127] Other creative researchers have even engineered melanin-loaded polymeric nanoparticles for use in PTT.[128,129]

The plethora of existing agents that have been reported can attest to the incredible amount of research effort dedicated to this topic. Unfortunately, there is inherent variability between different PT platforms relating to their intrinsic properties such as their extinction coefficients and PT conversion efficiencies, which are useful for determining the absorption cross section of the agent used.[130] However, additional factors such as the wide range of laser parameters and the diverse cancer models used must be considered just as carefully. As a result, a comparison between different PT agent platforms, or even across the same PT agent platform[81] is difficult, and does not yield meaningful conclusions (Table 1). For this reason, we opted to abstain from summarizing these studies in detail. Instead, we chose to highlight a few key milestone examples, as well as some trends in the development of this technique in Table 1, some of which we have already discussed above.

3.2 *Systemic Toxicity and the Challenge of Delivery*

Although unique agents are still being reported today, one issue that has persisted is the delivery of PT agents. PTT involving intratumoral (IT) routes of administration are still consistently outperforming intravenous (IV) ones. The necessity for direct injection into tumors can be problematic because of size, location, and the need to visualize the tumor and its borders with costly equipment, often in an operating or procedural room setting. Unfortunately, IV injection of PT agents, in addition to suffering from the disadvantage of poor accumulation in target tissues, also poses the potential problem of systemic toxicity. Recently, del Rosal et al.[131] reported on the application of $NdVO_4$ nanocrystals (NCs) for PTT. The authors observed an absorption cross section of 2.0×10^{-19} cm^2, which was eight orders of magnitude lower than gold's reported absorption cross section[85] of 2.93×10^{-11} cm^2. As a result, much more NCs were needed to achieve the desired absorption. The authors injected the NCs intratumorally at a concentration nearly 2000 times the maximum amount that they showed to be safe *in vitro* in order to achieve minimal PT heating that was only slightly more (~8°C) than the laser-alone group after 4 min of laser exposure. If the IT injected amount was diluted by the whole blood volume of the animal, which would be the case if the agent had been injected IV, the concentrations reached would still be an order of magnitude above the documented safety threshold shown by the authors. We then have to consider whether the PT agent itself could induce acute toxicity, not to mention the challenge associated with administering such a large amount of material. Ultimately, the general determining factor for toxicity of foreign agents is whether the concentrations injected are above the known acceptable thresholds for the therapeutic agents in question.[26] This means that PT agents with high absorptions but a low toxicity threshold could exhibit concerns, as well.

In general, one of the biggest concerns of nanoparticles is the fate of the nanoparticles after it is introduced into the body.[25–26,132] Ideally, injected NPs, especially those of an inorganic nature, should be renally cleared, which means that their hydrodynamic radii need to be less than 5.5 nm.[133–136] For this reason, the majority of IV injected inorganic nanoparticles are not approved by the FDA for systemic use clinically.[134] Unfortunately, almost all of the useful inorganic nanoparticle-based PT agents studied are above this accepted size range. When Sonavane et al.[137] investigated the biodistribution of gold nanoparticles of a broad size range (15 up to 200 nm), they found that 15 and 50 nm NPs were able to penetrate the blood brain barrier in mice. This result is alarming since the majority of gold nanoparticles used for PTT are in this size regime.[138] Nevertheless, some studies have shown that gold nanoparticles induced no acute toxicity when uptaken by human cells.[139]

The geometry of nanoparticles may also influence their biodistribution. Black et al.[140] investigated biodistribution of gold nanostructures with varying shapes and found that AuNRs and cages were distributed throughout tumors while nanospheres and nanodisks were around only the tumor periphery. In a similar study, Wang et al.[101] found that nanohexapods exhibited even higher cellular uptake, and more importantly, lower cytotoxicity compared to nanorods and nanocages of similar sizes, suggesting that geometry may also be implicated in the potential toxicity of nanoparticles. It is critical to ensure that injected nanoparticles are stable and structurally sound, especially because they can be easily heated to extreme temperatures due to their high-effective absorptions. Recently, Goodman et al.[141] reported on the surprising *in vivo* instability of hollow gold nanoshells (HGNSs). Although their HGNS were observed to be completely stable under laser irradiation in solution, biodistribution studies suggested that the nanoshells were heavily fragmented *in vivo*, with the authors attributing the cause of the

Table 1 Significant "milestone" in the development of PTT contributing to the progress in this field over the years.

Primary PT agent	Year	Cancer models	Method of administration	Light wavelength, power, and duration	Additional functionalities	Significance/commentary[a]
ICG	1995[22,189]	*In vivo*: DMBA-4 mammary xenograft, Wistar Furth rats	100 μL at 1% IT injection	808 nm, 3 to 5 W for 6 min or 15 W for 3 min, 3 mm spot diameter	N/A	First instance of "chromophore-enhanced tumor destruction"
AuNSs	2003[15]	*In vitro*: SK-BR-3 breast epithelial; *in vivo*: canine transmissible venereal tumor	*In vitro*: 4.4×10^9 particles/ml; *in vivo*: 20 to 50 μL IT injection	*In vitro*: 820 nm, 35 W/cm^2, 7 min; *in vivo*: 820 nm, 4 W/cm^2, 5 mm spot diameter, <6 min	Surface passivation with PEG	The term "PTT" is coined
AuNRs	2006[12]	*In vitro*: HaCaT (nonmalignant); HOC 313 clone 8 and HSC-3 (squamous cell carcinoma)	Incubation in $OD_{\lambda=800} = 0.5$ for 30 min followed by rinse	40, 80, 120, 160, and 200 mW, 1 mm spot diameter, 4 min	Polystyrene sulfonate coating; anti-EGFR monoclonal antibodies	"Selective" PT killing of cancer cells is demonstrated
AuNRs	2008[13]	HSC-3 human squamous cell carcinoma xenograft	IT: 15 μL at $OD_{\lambda=800} = 40$; IV: 100 μL at $OD_{\lambda=800} = 120$	IT: 0.9 to 1.1 W/cm^2, 6 mm spot diameter, 10 min; IV: 1.7 to 1.9 W/cm^2, 6 mm spot diameter, 10 min	Surface passivation with PEG	IT injection is more effective than IV, reiterating the challenge of "material confinement"
Graphene oxide nanosheets	2010[109]	*In vivo*: 4T1 tumor orthotopic xenograft on Balb/c mice	*In vivo*: 20 mg/kg IV injection followed by 24 h wait time before laser exposure	*In vivo*: 808 nm, 2 W/cm^2, 5 min	PEGylated and conjugated with Cy7, for in vivo imaging	More attention is paid to tumor uptake and systemic clearance
Transition metal di-chalcogenides (WS_2)	2014[181]	*In vitro*: 4T1, HeLa, 293T; *in vivo*: 4T1 tumor xenograft on Balb/c mice	*In vitro*: 0.1 mg/mL; *in vivo*: 2 mg/kg IT injection with 30 min wait; 20 mg/kg IV injection with 24 h wait	*In vitro*: 808 nm, 0.1 to 0.8 W/cm^2, 5 min; *in vivo*: 808 nm, 0.8 W/cm^2, 5 min	Lipoic acid-PEG functionalized; PAc and CT imaging	Challenge of material confinement is still not overcome; imaging modalities are incorporated
ICG/HSA NPs	2014[16]	4T1 breast cancer xenograft	0.5 mg ICG/kg equivalent of NPs IV injection	808 nm, 0.8 W/cm^2, 5 min; spot sized adjusted for different experiments	PDT; PAc imaging; fluorescence imaging	See Fig. 5; multiple modalities are added to PTT theranostic platforms
AuNRs and nanospheres	2016[5]	LoVo-6-Luc-1 colorectal cancer xenograft	6 mm hydrogel disks with 10 nM nanorods and spheres; or equivalent IT and IV doses	808 nm, 1 W, 120 s; applied on day 3, 4, 5, 10 after hydrogel implantation	Chemotherapy; gene therapy	See Fig. 4; more attention is paid to material and heat confinement

[a]To our knowledge, or in our opinion.

instability to residual silver ions remaining after synthesis of the HGNS. The findings are in line with what other researchers have observed for AuNRs, which are known to fragment or shorten upon exposure to high laser power densities, although smaller particles were found to be more resistant to fragmentation due to coupling to the environment.[103,142] Overall, these results are not unexpected, however, since systems often do not behave the same in aqueous dispersions as they do *in vivo*.[44] From these examples, we see that inorganic nanostructures still face many challenges before they can be translated into useful clinical therapies.[143]

Organic PT agents have not fared much better, mostly for the same reasons of biodistribution, stability, and toxicity related to processing.[25] For example, the high aspect ratio of carbon nanotubes, reminiscent of the geometry of carcinogens such as asbestos, led to long-term residence in the lungs of mice studied.[144] Residual metallic impurities from nanotube synthesis and undesirable aggregation are also commonly attributed to toxicity of carbon nanostructures.[132] Various strategies have been employed to functionalize PT agents with passivating polymers. Most commonly, polyethylene glycol (PEG) is employed to impart a stealth-like character to these agents to reduce their toxicity.[145,146] The attachment of targeting moieties to PT nanoparticle platforms for functional groups overexpressed in certain cancers may help improve the local accumulation of PT agents within the tumor to increase treatment specificity and hopefully their effectiveness, while also reducing their systemic toxicity (Table 1).[147]

Finally, the challenges of systemic delivery could be avoided altogether, if local routes of administration were developed and perfected. Conde et al.[5] recently reported on a well-characterized triple-combination PT, chemo, and gene therapy applied at the tumor location in the form of a hydrogel patch with or without tumor resection (Fig. 4). In their prophylaxis study without preresection, a hydrogel patch loaded with gold nanoparticles and nanorods was implanted 15 days after tumor induction, with multiple PT treatment events starting on day 18. The remarkable part of this study was in its methodology. Instead of choosing traditional PTT methods involving a single exposure at a high power density, the authors opted for multiple treatment events of short durations (120 s) applied once per day over the span of several days. Although the authors did not discuss their reasoning for the short exposure times, these times corresponded well, and likely not by coincidence, to the thermal relaxation times we calculated in Sec. 2 for the corresponding tumor sizes in this study. This prophylactic triple combination treatment, which is especially relevant for nonresectable tumors, was able to achieve complete tumor remission, whereas the control group with tumor resection saw only 40% tumor recurrence. Furthermore, treatment following IT or systemic injection of the gold nanomaterials resulted in only 60% and 40% tumor reduction, respectively. This result is consistent with most of the existing studies comparing IT and IV modes of administration.[148,149] Strategies such as this could help reduce the chance for systemic toxicity, although it would be important to ensure that the PT agents did not extravasate elsewhere. However,

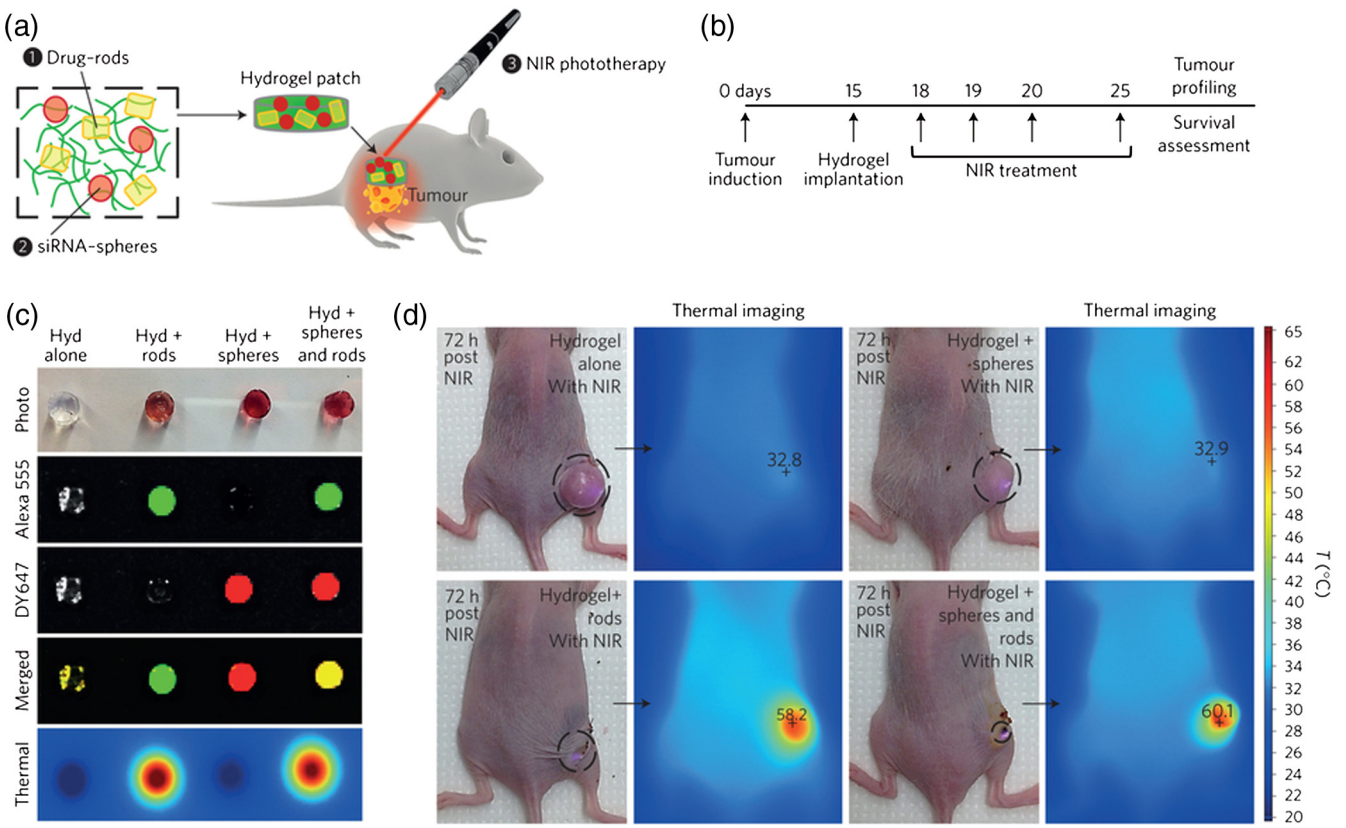

Fig. 4 A triple-combination local delivery platform developed by Conde et al., in which chemotherapy, genetherapy, and PTT are applied in conjunction to eradicate cancer. For the PTT component of the treatment, the authors performed four sessions of laser exposure for 120 s each (1 W, 808 nm) on days 18, 19, 20, and 25 to reach temperatures as high as 60°C to damage colorectal cancer in a xenograft tumor model in mice. Reprinted with permission from Macmillan Publishers Ltd. Ref. 5, © 2016.

choosing known low-toxicity agents with well-documented excretion pathways can obviate some of these concerns.

In this section, we saw that a significant amount of effort has been dedicated toward finding agents with high effective absorptions for PTT. However, the potential systemic toxicity of PT agents and their route of administration are factors that must also be carefully considered regardless of the effective absorption of the agent. In Sec. 2, we suggested that one possible way the parameters of light exposure could be optimized is to limit the heating to tumors, while sparing surrounding tissues. In this section, we saw a recent example of researchers already moving forward in that direction. In the next sections, we discuss in more detail, how nanomedicine[150–153] has helped and may continue to help mitigate attenuation effects resulting from improperly introduced PT agents and address toxicity concerns.[154,155]

4 Nanomedicine Enabled Synergistic Photothermal Therapy Platforms

PTT, as we have presented so far, involves light-induced heating to high temperatures with the assistance of strongly absorbing PT agents to ablate cancerous tissues. Apart from being used to directly ablate tumors cells, light induced heating is useful in many other processes related to cancer therapy, as well. In this section, we present some examples, in which PT agents are integrated with other cancer therapeutic or imaging modalities to garner multifunctional theranostic nanoparticle delivery platforms to enhance the outcome of cancer treatment.

4.1 *Benefits of Mild Hyperthermia*

Hyperthermia involves heating of biological tissues to physiologically irregular temperatures. While temperatures above 43°C are employed to ablate tissue, heating to milder temperatures could also prove to be beneficial in the context of cancer therapy.[156–158] One of the first responses by the body to local hyperthermia is enhanced blood flow to the region to dissipate heat. As mentioned in Sec. 1, the tortuous nature of the improperly formed blood vessels found in tumors creates a selective mechanism for heat build-up. This property, combined with the typically lower threshold of tumor cells to tolerate heat, naturally make tumors more susceptible to thermal damage.[20] Increased blood flow also contributes to amplifying the EPR effect to enhance the amount of material accumulating in the tumor,[159] such as circulating PT agents or chemotherapy drugs, perhaps all loaded into and delivered by a single nanoconstruct. Mild temperature elevations may also trigger subcellular events to render cells susceptible to damage through apoptosis.[23,106,158,160] In addition, it may drive a shift toward anaerobic metabolism in cells, resulting in higher oxygen availability to the tissue environment to overcome the hypoxic conditions typically found in tumors that have limited the efficacy of oxygen-dependent cancer therapies.[127,161] Unfortunately, one major undesirable heating-associated effect is the activation of immunological responses, including the upregulation of heat shock proteins (Hsp)[162] that lends itself to protect cancer cells from being damaged.[163,164] In fact, studies have shown that the ability of cancers to upregulate Hsp production is well correlated with the aggressiveness of the cancer,[162] resulting in various gene therapy-based strategies to block Hsp production to improve cancer treatment outcomes.[113,165] Nevertheless, by integrating PT capabilities into theranostic nanoparticle platforms, researchers could use the mild heating regime to initially amplify the efficacy of other treatment modalities, followed by controlled PT ablation at higher laser power densities, creating a two-pronged attack, to help to ensure tumor destruction.

4.2 *Photothermally Triggered Payload Release*

Controlled drug release is important in cancer chemotherapy because it enables potent chemotherapeutic drugs to kill the cancers while minimizing systematic toxicity. Many physical, chemical, and physiological signals have been explored to act as triggers for controlled release of chemotherapy drugs. As discussed previously, light is a unique trigger but is still limited by the availability of effective photochemical processes. In addition to synergistic enhancement of other therapies, heating, generated by PT agents with the irradiation of light, can expand the utility of light-controlled release to nonphotoresponsive systems. In general, various drug carriers such as liposomes,[166] polyelectrolyte capsules, polymeric nanoparticles,[75] and even blood-cell-mimicking capsules[167] all become less stable and more permeable upon heating, leading to the therapeutic cargo eluting from their interior. Moreover, the burst nature of heating-induced release can effectively enhance the efficacy of treatments such as chemotherapy in the appropriate environment. Following this concept, various studies using laser-triggered controlled release systems involving PT transducers and thermoresponsive systems or phase-changing materials as release substrate have been demonstrated.[168–170] In one example, Kim et al. reported an elegant system utilizing AuNSs for the photothermally triggered cargo release. They first load the cargo into liposomes and encapsulate the liposomes with a thin layer of the nanoshells. The integrity of the AuNSs make the liposome leakage-free under ambient conditions. Upon the exposure to NIR light, the AuNSs generated heating via the PT effect and deform *in situ*, triggering the release of cargo from the interior.[171] In a similar example, Zheng et al.[169] designed a synergistic chemo/PTT platform containing the common chemotherapy agent, doxorubicin (DOX), and ICG loaded into a lipid–polymer nanoparticle system (DINP). The authors showed that the DINPs were stable in the absence of light, but with a single, 8-min treatment of 808-nm laser at 1 W/cm^2, they were able to trigger the release of DOX and also heat the tumor to more than 50°C to ablate it. Compared to the all of the controls, the DINPs were the most effective and seemed to be the only system able to suspend tumor growth for up to 17 days. Although not applied to cancer, our own research group recently demonstrated the exciting potential for using selective PT heating of water nanodomains confined inside nonlight responsive polymer microparticles, as a means to induce payload release.[75]

4.3 *Photothermally Enhanced Cellular Uptake*

PT heating could also be leveraged to increase cellular uptake, as well.[172] It is known that many nanosized objects are uptaken by cells via receptor-mediated endocytosis, macropinocytosis, and other membrane-related processes. A number of studies have shown that the permeability of cell membrane can be significantly enhanced when the environmental temperature is increased to 43°C, resulting in the uptake of more therapeutic agents in the targeted regime.[173] Provided that most therapeutic agents require a minimum concentration to be effective, enhancing localized uptake to cells may potentially increase the utilization percentage of delivered therapeutic agents, while lowering the overall dose that needs to be administered.[44] Following this

concept, Sherlock et al. demonstrated that ultrasmall iron-cobalt (FeCo)-core–graphitic-carbon-shell nanoparticles loaded with the DOX exhibited accelerated cellular uptake upon NIR laser irradiation.[174] Particularly, the FeCo-graphitic-shell nanoparticles with a large absorption band can heat the targeted cells from 37°C to 43°C at laser power densities as low as 0.3 W/cm^2. The 6°C incremental temperature increase in the cell media induced a two-fold increase in the cellular uptake of the FeCo-graphitic-shell nanoparticles loaded with DOX. Similarly, Tian et al.[108] showed that the uptake of nanographene, which has proven to be an effective carrier for gene transfection without any other aids, can be enhanced three-fold with NIR exposure. The Lapotko group also demonstrated an intriguing pathway of applying the PT effect for enhanced drug delivery. They found that plasmonic noble metal nanoparticles exposed to short laser pulses could generate transient vapor bubbles which could adhere to cell membranes and disrupt them upon the burst of these bubbles. The authors demonstrated that the burst event can be used either as a trigger for drug release from the carrier or to enhance endosome escape of the engulfed drugs.[175] These strategies to enhance cell membrane permeability are promising and are likely to become more popular in translational nanomedicine research because many of the drug delivery vehicles could be engineered to have these capabilities.

4.4 *Combination Phototherapies*

Combinatorial therapies that integrate several therapeutic approaches together, such as the PTT/chemotherapy system described above,[174] have generally proven to be more effective than stand-alone techniques.[176] PDT is an oxygen-dependent light-based cancer therapy very similar to PTT, in which photosensitizer molecules transfer the energy of the absorbed photon to the surrounding molecular oxygen to locally generate toxic singlet oxygen molecules, instead of heat, resulting in local toxicity to effectively damage the structure and function of cancer cells. Like PTT, PDT has many of the same advantages of high specificity and low systemic toxicity compared to conventional chemotherapy. However, an inevitable drawback that has hindered the efficacy of PDT in tumor treatment is its requirement for oxygen. The hypoxic conditions found inside tumors are exacerbated by the depletion of the already limited oxygen supply from the oxygen-consuming reactions of PDT. It is also important to isolate PDT agents inside drug delivery vehicles because these highly sensitive species could become toxic with exposure to even ambient levels of light.[177] Nevertheless, due to the high level of similarity between PDT and PTT, it made sense to design systems with both modes of therapy integrated. Jang et al. demonstrated an interesting example by using AuNRs as both carrier and quencher for the PDT agent, aluminum phthalocyanine tetrasulfonate ($AlPcS_4$). $AlPcS_4$ was assembled onto the surface of AuNRs and quenched by the surface plasmon resonance. Therefore, they were nonphototoxic even when exposed to light of proper wavelengths. Only when the AuNRs were used to generate heat under laser irradiation were the photosensitizers released from the surface, thus becoming phototoxic. In a similar example, gold nanostars were surface functionalized with another PDT agent, chlorin e-6, to perform dual PDT/PTT.[98] In concept, PDT initially performs according to its design parameters due to the presence of oxygen, but as oxygen becomes depleted, PTT takes over as the predominant mode of tumor damage, and in combination, conspires to doubly damage the tumor.

4.5 *Photothermal Therapy/Photoacoustic Imaging*

Adding diagnostic functions to nanoparticle drug delivery systems can be useful for tracking their location, as well as help provide information and feedback regarding the therapy. Photoacoustic (PAc) imaging, a natural "derivative" of the PT effect, is likely the easiest to implement along with PTT because it utilizes the heat generated from laser irradiation to produce acoustic waves that can convey both the anatomic and functional information about the tissues probed.[178,179] Huang et al.[180] reported a biodegradable gold nanovesicle composed of a simple design comprised of PEG-b-PCL tethered to AuNPs for PAc imaging and PTT, simultaneously, while under the irradiation of the same laser. More recently, Yong et al.[181] and Song et al.[182] reported using WS_2 quantum dots and two-dimensional Co_9Se_8 nanosheets, respectively, as agents for both PTT and PAc imaging. These materials belong to a group of PT agents classified as metal chalcogenides,[183–186] which exhibit broad absorption spectra, high extinction coefficients, and PT conversion efficiencies, as well as low cytotoxicity.[187] Moreover, these nanostructures can be easily functionalized to enable other popular imaging modalities, such as fluorescence imaging, magnetic resonance imaging,[188] and computed tomography,[181] without affecting the PT conversion process, thereby making them even more powerful as platforms for PT applications.

5 Progress and Future Perspectives

5.1 *Case Study: Indocyanine Green Then and Now*

Through the examples presented thus far, it is evident that PTT has progressed significantly since the idea of light-induced heating to kill cancer was first conceptualized. To provide some perspective, we present, to our knowledge, one of the earliest examples of PTT, or "chromophore-enhanced tumor destruction," as it was referred to in 1995 (Table 1).[22] After having characterized their system *in vitro*,[189] Chen et al. subcutaneously injected 0.5% to 1% ICG in free dye form, into mammary fat-pad tumors of rats, exposed them to various laser power densities, and monitored the animals for up to 9 days. Several important conclusions were drawn from this study which reiterates many of the challenges for PTT presented thus far. First, the authors found that laser powers in the 3- to 5-W range worked unequivocally better than higher powers in the 10- to 15-W range, since the higher powers rapidly denatured and burned tissue, creating a carbonized tissue layer that effectively shielded NIR light from penetrating into tissue, suggesting that the parameters of light exposure must be carefully considered. Second, the authors conceded that the model showed efficacy, likely because IT administration of the dye into the capsule-like tumor allowed the chromophore to be sequestered long enough to allow for PT treatment, suggesting that encapsulation, delivery, and accumulation of PT agents, especially small molecule dyes like ICG, via alternate routes of administration, might be critical to the success of PTT. Finally, the authors found that although tumor destruction was apparent in their period of observation, a sufficient amount of tumor cells remained viable and was able to perpetuate the tumor growth in all of groups. A study extending out to 30 days revealed that at time of death, the laser-ICG treated tumors were still about half the size of tumors treated by lasers only.[190] This result suggested that PTT alone, at least as a single treatment, may not be sufficient in eradicating a tumor. Cancer has proven to be a complex and formidable challenge for medical

sciences. Multipronged strategies involving therapies such as PTT at specified times and parameters, following surgical interventions such as reduction of tumor bulk combined with other modalities such as chemo, radiation, immunotherapy, and stem cell targeting, are likely needed to improve treatment outcomes.

In this review, we have highlighted significant advances in nanomedicine; over the past two decades, researchers in many fields have helped us understand and overcome many challenges. As an example, a simple yet elegant system, comprising ICG as the primary photosensitizer, was recently reported by Sheng et al. (Fig. 5).[16] ICG, in addition to being applied for PTT, and by extension, PAc imaging, can also serve as a photosensitizer in PDT when exposed to low-power short-term laser exposures.[191,192] The authors attached ICG to human serum albumin (HSA) using thiol chemistry, and the system subsequently self-assembled into a theranostic nanoparticle platform (HSA-ICG NP).[16] By formulating ICG into NPs, they were able to enhance its uptake into cancer cells in addition to improving the stability of the dye in terms of its rapid clearance and photobleaching, while also enabling fluorescence imaging. The authors intravenously injected the HAS-ICG-NPs and in terms of imaging, were able to track the NPs through dual PAc/fluorescence imaging. In terms of therapy, they were able to deliver the ICG-NPs, as well as achieve dual PDT/PTT, by applying an 808-nm laser continuously for 5 min at 0.8 W/cm^2. In the xenograft model, this combined therapy was able to completely destroy the tumor and ensure the survival of all the animals in the study group, out to 50 days, while only stunted tumor growth was observed in all of the control groups (particles alone, laser alone, or interval exposure), with no animals surviving beyond 25 days. Interestingly, when the same study was carried out in an orthotopic tumor model with the same type of cancer (4T1 breast carcinoma), interval exposure was able to prolong the survival of the animals an additional 10 days, out to 35 days, while other control groups of particles alone or laser alone performed about the same as the xenograft study, demonstrating at least some degree of effectiveness akin to SPT with interval exposure. The reduced effectiveness for the interval group compared to the continuous exposure group could be attributed to the long rest times between exposure events (1 min exposures with 5 min rest intervals) in the interval exposure group. Overall, compared to the work by Chen et al., this work involved only a single photosensitizing agent, and it was still able to accomplish tumor destruction through dual therapy and also provide diagnostic information by tracking the injected nanoparticles.

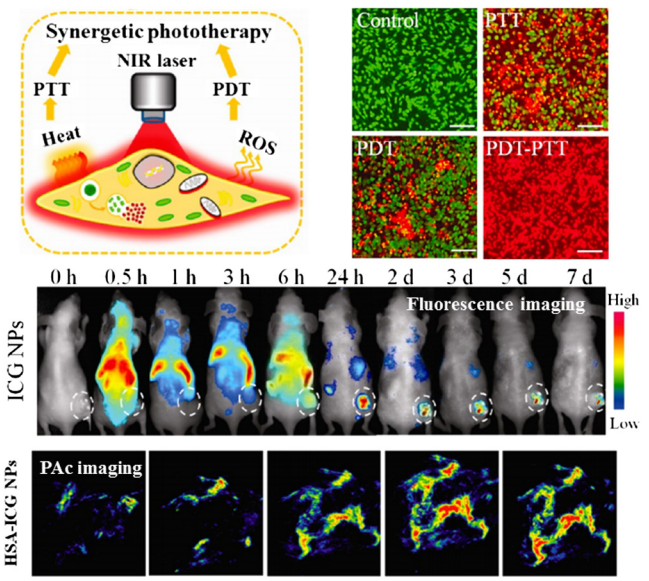

Fig. 5 PT theranostic systems such as indocyanine-HSA nanoparticles are capable of multimodal imaging, as well as multimodal therapy to allow for the tracking of the PT agents in conjunction with combination therapy to improve cancer treatment outcomes.[16] Adapted with permission from the American Chemical Society © 2016.

5.2 *Concluding Remarks*

The development of various engineered NIR-light-absorbing nanoscale agents will continue to attract attention in the field of cancer therapy and beyond. In this review, we presented many examples of how PTT has incrementally evolved over the years. The idea of applying the PT effect to treat cancer arguably arose from the desire to expand upon the therapeutic benefits of mild hyperthermia therapy. As vast libraries of powerful PT agents were developed, PTT research deviated from mild hyperthermia therapy and evolved into ablation therapy, where high laser powers were used to heat up these highly efficient agents to uncontrollably damage tissue. However, as researchers began to understand the implications of uncontrolled heating, attention began to shift toward carefully controlling the light-exposure to achieve more defined thermal damage. There was also a shift back toward applying the PT effect to achieve mild hyperthermia to synergistically bolster other treatment modalities in cancer therapy. Although our review is far from being exhaustive, present efforts support this claim and indicate continued development and refinement of some of the more complex theranostic PT platforms incorporating PT agents of all types for use in multiple imaging and therapeutic applications. The addition of targeting capabilities to improve accumulation of nanoparticle therapeutic platforms within tissues of interest, as well as selective heat confinement through controlled light exposure, are strategies vital to expanding the ability of this platform to assist preclinical and clinical research. The field of nanomedicine has helped tremendously on the material-confinement front. Looking forward, careful manipulation of the parameters of light exposure, perhaps through concepts borrowed from SPT theory, could push a shift in paradigm in this field that may one day lead to truly selective heating of tumors, which if achieved, would bring PTT one step closer to becoming a vital prong in the clinical cancer therapy approach.

Disclosures

The authors have no financial interests or other conflicts of interest to disclose at this time.

Acknowledgments

The authors would like to thank Dr. Paul Chasan and Dr. Amy Moore for their comments and suggestions during editing of this work. The authors would also like to thank the National Institutes of Health (National Eye Institute, NEI) Award No. R01EY024134 and the Air Force Office of Scientific Research (AFOSR) Award No. FA9550-15-1-0273 for funding.

References

1. S. L. Murphy, J. Xu, and K. D. Kochanek, "Deaths: final data for 2010," in *National Vital Statistics Reports: From the Centers for Disease Control and Prevention*, National Center for Health Statistics, National Vital Statistics System, Vol. 61, pp. 1–117 (2013).
2. R. L. Siegel, K. D. Miller, and A. Jemal, "Cancer statistics, 2015," *CA Cancer J. Clin.* **65**, 5–29 (2015).
3. G. J. Slotman, C. H. Doolittle, and A. S. Glicksman, "Preoperative combined chemotherapy and radiation therapy plus radical surgery in advanced head and neck cancer. Five-year results with impressive complete response rates and high survival," *Cancer* **69**, 2736–2743 (1992).
4. H. Cho et al., "A phase 2 trial of radiation therapy with concurrent paclitaxel chemotherapy after surgery in patients with high-risk endometrial cancer: a Korean gynecologic oncologic group stud," *Int. J. Radiat. Oncol. Biol. Phys.* **90**, 140–146 (2014).
5. J. Conde et al., "Local triple-cominbation therapy results in tumour regression and prevents recurrence in a colon cancer model," *Nat. Mater.* **15**, 1128–1138 (2016).
6. D. Lorusso et al., "A systematic review comparing cisplatin and carboplatin plus paclitaxel-based chemotherapy for recurrent or metastatic cervical cancer," *Gynecol. Oncol.* **133**, 117–123 (2014).
7. O. Caffo et al., "Gemcitabine and radiotherapy plus cisplatin after transurethral resection as conservative treatment for infiltrating bladder cancer: long-term cumulative results of 2 prospective single-institution studies," *Cancer* **117**, 1190–1196 (2011).
8. B. Diop et al., "Mesenteric myofibroblastic tumor: NSAID therapy after incomplete resection," *J. Visc. Surg.* **148**, e311–e314 (2011).
9. A. Faggiano et al., "A decrease of calcitonin serum concentrations less than 50 percent 30 minutes after thyroid surgery suggests incomplete C-cell tumor tissue removal," *J. Clin. Endocrinol. Metab.* **95**, E32–E36 (2010).
10. C. A. Metildi et al., "Fluorescence-guided surgery of pancreatic cancer using activatable cell penetrating peptides (ACPPs) in orthotopic mouse models," *Ann. Surg. Oncol.* **21**, 1405–1411 (2014).
11. E. Y. Lukianova-Hleb et al., "Intraoperative diagnostics and elimination of residual microtumours with plasmonic nanobubbles," *Nat. Nanotechnol.* **11**, 525–532 (2016).
12. X. H. Huang et al., "Cancer cell imaging and photothermal therapy in the near-infrared region by using gold nanorods," *J. Am. Chem. Soc.* **128**, 2115–2120 (2006).
13. E. B. Dickerson et al., "Gold nanorod assisted near-infrared plasmonic photothermal therapy (PPTT) of squamous cell carcinoma in mice," *Cancer Lett.* **269**, 57–66 (2008).
14. X. H. Zheng et al., "Indocyanine green-containing nanostructure as near infrared dual-functional targeting probes for optical imaging and photothermal therapy," *Mol. Pharm.* **8**, 447–456 (2011).
15. L. R. Hirsch et al., "Nanoshell-mediated near-infrared thermal therapy of tumors under magnetic resonance guidance," *Proc. Natl. Acad. Sci. U. S. A.* **100**, 13549–13554 (2003).
16. Z. H. Sheng et al., "Smart human serum albumin-indocyanine green nanoparticles generated by programmed assembly for dual-modal imaging-guided cancer synergistic phototherapy," *ACS Nano* **8**, 12310–12322 (2014).
17. G. Lamouche et al., "Review of tissue simulating phantoms with controllable optical, mechanical and structural properties for use in optical coherence tomography," *Biomed. Opt. Express* **3**, 1381–1398 (2012).
18. T. M. Zagar et al., "Hyperthermia combined with radiation therapy for superficial breast cancer and chest wall recurrence: a review of the randomised data," *Int. J. Hyperthermia* **26**, 612–617 (2010).
19. P. S. Yarmolenko et al., "Thresholds for thermal damage to normal tissues: an update," *Int. J. Hyperthermia* **27**, 320–343 (2011).
20. K. F. Chu and D. E. Dupuy, "Thermal ablation of tumours: biological mechanisms and advances in therapy," *Nat. Rev. Cancer* **14**, 199–208 (2014).
21. N. R. Datta et al., "Hyperthermia and radiation therapy in locoregional recurrent breast cancers: a systematic review and meta-analysis," *Int. J. Radiat. Oncol. Biol. Phys.* **94**, 1073–1087 (2016).
22. W. R. Chen et al., "Chromophore-enhanced in-vivo tumor-cell destruction using an 808-nm diode-laser," *Cancer Lett.* **94**, 125–131 (1995).
23. J. R. Melamed, R. S. Edelstein, and E. S. Day, "Elucidating the fundamental mechanisms of cell death triggered by photothermal therapy," *ACS Nano* **9**, 6–11 (2015).
24. P. A. Valdes et al., "A spectrally constrained dual-band normalization technique for protoporphyrin IX quantification in fluorescence-guided surgery," *Opt. Lett.* **37**, 1817–1819 (2012).
25. S. Sharifi et al., "Toxicity of nanomaterials," *Chem. Soc. Rev.* **41**, 2323–2343 (2012).
26. E. Casals et al., "Distribution and potential toxicity of engineered inorganic nanoparticles and carbon nanostructures in biological systems," *TrAC Trends Anal. Chem.* **27**, 672–683 (2008).
27. T. Gould, Q. Wang, and T. J. Pfefer, "Optical-thermal light-tissue interactions during photoacoustic breast imaging," *Biomed. Opt. Express* **5**, 832–847 (2014).
28. S. Guizard et al., "Interaction of short and intense light pulses with matter: visible versus VUV," *Proc. SPIE* **6586**, 65860F (2007).
29. Y. Joly, "Interaction of polarized light with matter," *Magn. Synchrotron Radiat. New Trends* **133**, 77–125 (2010).
30. P. J. Wu and J. T. Walsh Jr., "Stokes polarimetry imaging of rat tail tissue in a turbid medium: degree of linear polarization image maps using incident linearly polarized light," *J. Biomed. Opt.* **11**, 014031 (2006).
31. B. Cox, *Laser–Tissue Interactions*, Lecture Notes. Unpublished (2013).
32. S. D. Bianco, F. Martelli, and G. Zaccanti, "Penetration depth of light re-emitted by a diffusive medium: theoretical and experimental investigation," *Phys. Med. Biol.* **47**, 4131–4144 (2002).
33. A. Pifferi et al., "New frontiers in time-domain diffuse optics, a review," *J. Biomed. Opt.* **21**, 091310 (2016).
34. J. R. Weber et al., "Multispectral imaging of tissue absorption and scattering using spatial frequency domain imaging and a computed-tomography imaging spectrometer," *J. Biomed. Opt.* **16**, 011015 (2011).
35. H. Duadi and D. Fixler, "Influence of multiple scattering and absorption on the full scattering profile and the isobaric point in tissue," *J. Biomed. Opt.* **20**, 056010 (2015).
36. H. W. Wang et al., "Broadband reflectance measurements of light penetration, blood oxygenation, hemoglobin concentration, and drug concentration in human intraperitoneal tissues before and after photodynamic therapy," *J. Biomed. Opt.* **10**, 014004 (2005).
37. Z. Huang, "A review of progress in clinical photodynamic therapy," *Technol. Cancer Res. Treat.* **4**, 283–293 (2005).
38. B. Bahmani et al., "Functionalized polymeric nanoparticles loaded with indocyanine green as theranostic materials for targeted molecular near infrared fluorescence imaging and photothermal destruction of ovarian cancer cells," *Laser Surg. Med.* **46**, 582–592 (2014).
39. Y. Lv et al., "Conjugated polymer-based hybrid nanoparticles with two-photon excitation and near-infrared emission features for fluorescence bioimaging within the biological window," *ACS Appl. Mater. Interfaces* **7**, 20640–20648 (2015).
40. H. Chen et al., "Understanding the photothermal conversion efficiency of gold nanocrystals," *Small* **6**, 2272–2280 (2010).
41. Z. Zha et al., "Uniform polypyrrole nanoparticles with high photothermal conversion efficiency for photothermal ablation of cancer cells," *Adv. Mater.* **25**, 777–782 (2013).
42. X. Liu et al., "Facile synthesis of biocompatible cysteine-coated CuS nanoparticles with high photothermal conversion efficiency for cancer therapy," *Dalton Trans.* **43**, 11709–11715 (2014).
43. J. M. Schurr, "Interaction of light-pulses with matter.: 1. Derivation of Beer–Lambert law," *Chem. Phys.* **15**, 1–13 (1976).
44. A. Espinosa et al., "Cancer cell internalization of gold nanostars impacts their photothermal efficiency in vitro and in vivo: toward a plasmonic thermal fingerprint in tumoral environment," *Adv. Healthcare Mater.* **5**, 1040–1048 (2016).
45. M. Oda et al., "Quantitation of absolute concentration change in scattering media by the time-resolved microscopic Beer–Lambert law," *Adv. Exp. Med. Biol.* **345**, 861–870 (1994).
46. H. Zhang et al., "Time integrated spectroscopy of turbid media based on the microscopic Beer–Lambert law: application to small-size phantoms having different boundary conditions," *J. Biomed. Opt.* **4**, 183–190 (1999).
47. A. W. Sainter, T. A. King, and M. R. Dickinson, "Effect of target biological tissue and choice of light source on penetration depth and resolution in optical coherence tomography," *J. Biomed. Opt.* **9**, 193–199 (2004).
48. I. S. Sidorov et al., "Estimation of light penetration depth in turbid media using laser speckles," *Opt. Express* **20**, 13692–13701 (2012).

49. P. Avci et al., "Low-level laser (light) therapy (LLLT) in skin: stimulating, healing, restoring," *Semin. Cutan. Med. Surg.* **32**, 41–52 (2013).
50. S. H. Tseng et al., "Chromophore concentrations, absorption and scattering properties of human skin in-vivo," *Opt. Express* **17**, 14599–14617 (2009).
51. N. Kollias and A. H. Baqer, "Absorption mechanisms of human melanin in the visible, 400–720 nm," *J. Invest. Dermatol.* **89**, 384–388 (1987).
52. P. Corcuff et al., "Skin optics revisited by in vivo confocal microscopy: melanin and sun exposure," *J. Cosmet. Sci.* **52**, 91–102 (2001).
53. O. Fasugba, A. Gardner, and W. Smyth, "The Fitzpatrick skin type scale: a reliability and validity study in women undergoing radiation therapy for breast cancer," *J. Wound Care* **23**, 358–368 (2014).
54. P. J. Matts, P. J. Dykes, and R. Marks, "The distribution of melanin in skin determined in vivo," *Br. J. Dermatol.* **156**, 620–628 (2007).
55. N. Kollias, "The absorption properties of 'physical' sunscreens," *Arch. Dermatol.* **135**, 209–210 (1999).
56. A. I. Dragan and C. D. Geddes, "Excitation volumetric effects (EVE) in metal-enhanced fluorescence," *Phys. Chem. Chem. Phys.* **13**, 3831–3838 (2011).
57. K. Ahrar et al., "Preclinical assessment of a 980-nm diode laser ablation system in a large animal tumor model," *J. Vasc. Interventional Radiol.* **21**, 555–561 (2010).
58. V. A. Dubinskaya et al., "Comparative study of the state of water in various human tissues," *Bull. Exp. Biol. Med.* **144**, 294–297 (2007).
59. T. E. Cooper and G. J. Trezek, "Correlation of thermal properties of some human tissue with water content," *Aerosp. Med.* **42**, 24–27 (1971).
60. R. Medvid et al., "Current applications of MRI-guided laser interstitial thermal therapy in the treatment of brain neoplasms and epilepsy: a radio logic and neurosurgical overview," *Am. J. Neuroradiol.* **36**, 1998–2006 (2015).
61. G. Zaccanti et al., "Optical properties of biological tissues," *Proc. SPIE* **2359**, 513 (1995).
62. S. L. Jacques, "Optical properties of biological tissues: a review," *Phys. Med. Biol.* **58**, R37–R61 (2013).
63. Q. Ju et al., "An upconversion nanoprobe operating in the first biological window," *J. Mater. Chem. B* **3**, 3548–3555 (2015).
64. M. Haedersdal and H. C. Wulf, "Evidence-based review of hair removal using lasers and light sources," *J. Eur Acad. Dermatol.* **20**, 9–20 (2006).
65. C. Dierickx, M. B. Alora, and J. S. Dover, "A clinical overview of hair removal using lasers and light sources," *Dermatol. Clin.* **17**, 357–366 (1999).
66. M. Heger et al., "Laser-induced primary and secondary hemostasis dynamics and mechanisms in relation to selective photothermolysis of port wine stain," *J. Dermatol. Sci.* **63**, 139–147 (2011).
67. L. Oguzkurt, "Endovenous laser ablation for the treatment of varicose veins," *Diagn. Interv. Radiol.* **18**, 417–422 (2012).
68. I. Golbasi et al., "Endovenous laser with miniphlebectomy for treatment of varicose veins and effect of different levels of laser energy on recanalization. A single center experience," *Laser Med. Sci.* **30**, 103–108 (2015).
69. R. R. Anderson and J. A. Parrish, "Selective photothermolysis: precise microsurgery by selective absorption of pulsed radiation," *Science* **220**, 524–527 (1983).
70. G. B. Altshuler et al., "Extended theory of selective photothermolysis," *Lasers Surg. Med.* **29**, 416–432 (2001).
71. P. E. Dyer, M. E. Khosroshahi, and S. J. Tuft, "Studies of laser-induced cavitation and tissue ablation in saline using a fiber-delivered pulsed HF laser," *Appl. Phys. B* **56**, 84–93 (1993).
72. W. Sheng et al., "Gold nanoparticle-assisted selective photothermolysis of adipose tissue (NanoLipo)," *Plast. Reconstr. Surg.* **2**, e283 (2014).
73. I. Y. Yanina et al., "Fat tissue histological study at indocyanine green-mediated photothermal/photodynamic treatment of the skin in vivo," *J. Biomed. Opt.* **17**, 058002 (2012).
74. B. C. Gulack et al., "The impact of tumor size on the association of the extent of lymph node resection and survival in clinical stage I non-small cell lung cancer," *Lung Cancer* **90**, 554–560 (2015).
75. M. L. Viger et al., "Near-infrared-induced heating of confined water in polymeric particles for efficient payload release," *ACS Nano* **8**, 4815–4826 (2014).
76. S. Ghosh et al., "Increased heating efficiency and selective thermal ablation of malignant tissue with DNA-encased multiwalled carbon nanotubes," *ACS Nano* **3**, 2667–2673 (2009).
77. P. K. Jain et al., "Calculated absorption and scattering properties of gold nanoparticles of different size, shape, and composition: applications in biological imaging and biomedicine," *J. Phys. Chem. B* **110**, 7238–7248 (2006).
78. M. Hu et al., "Gold nanostructures: engineering their plasmonic properties for biomedical applications," *Chem. Soc. Rev.* **35**, 1084–1094 (2006).
79. L. C. Kennedy et al., "A new era for cancer treatment: gold-nanoparticle-mediated thermal therapies," *Small* **7**, 169–183 (2011).
80. X. Huang et al., "Gold nanoparticles: interesting optical properties and recent applications in cancer diagnostics and therapy," *Nanomedicine* **2**, 681–693 (2007).
81. R. Vankayala et al., "Gold nanoshells-mediated bimodal photodynamic and photothermal cancer treatment using ultra-low doses of near infra-red light," *Biomaterials* **35**, 5527–5538 (2014).
82. E. C. Dreaden et al., "The golden age: gold nanoparticles for biomedicine," *Chem. Soc. Rev.* **41**, 2740–2779 (2012).
83. W. Cai et al., "Applications of gold nanoparticles in cancer nanotechnology," *Nanotechnol. Sci. Appl.* **2008**, 17–32 (2008).
84. M. Chen et al., "Polypyrrole nanoparticles for high-performance in vivo near-infrared photothermal cancer therapy," *Chem. Commun.* **48**, 8934–8936 (2012).
85. P. K. Jain et al., "Calculated absorption and scattering properties of gold nanoparticles of different size, shape, and composition: applications in biological imaging and biomedicine," *J. Phys. Chem. B* **110**, 7238–7248 (2006).
86. X. Liu et al., "Extinction coefficient of gold nanoparticles with different sizes and different capping ligands," *Colloids Surf. B* **58**, 3–7 (2007).
87. K. Jiang, D. A. Smith, and A. Pinchuk, "Size-dependent photothermal conversion efficiencies of plasmonically heated gold nanoparticles," *J. Phys. Chem. C* **117**, 27073–27080 (2013).
88. S. Link and M. A. El-Sayed, "Size and temperature dependence of the plasmon absorption of colloidal gold nanoparticles," *J. Phys. Chem. B* **103**, 4212–4217 (1999).
89. S. Link, M. B. Mohamed, and M. A. El-Sayed, "Simulation of the optical absorption spectra of gold nanorods as a function of their aspect ratio and the effect of the medium dielectric constant," *J. Phys. Chem. B* **103**, 3073–3077 (1999).
90. B. Nikoobakht and M. A. El-Sayed, "Preparation and growth mechanism of gold nanorods (NRs) using seed-mediated growth method," *Chem. Mater.* **15**, 1957–1962 (2003).
91. J. Fang, H. Nakamura, and H. Maeda, "The EPR effect: unique features of tumor blood vessels for drug delivery, factors involved, and limitations and augmentation of the effect," *Adv. Drug Delivery Rev.* **63**, 136–151 (2011).
92. S. T. Wilhelm et al., "Analysis of nanoparticle delivery to tumours," *Nat. Rev. Mater.* **1**, 16014 (2016).
93. U. S. Chung et al., "Dendrimer porphyrin-coated gold nanoshells for the synergistic combination of photodynamic and photothermal therapy," *Chem. Commun.* **52**, 1258–1261 (2016).
94. R. D. Averitt, S. L. Westcott, and N. J. Halas, "Linear optical properties of gold nanoshells," *J. Opt. Soc. Am. B* **16**, 1824–1832 (1999).
95. S. J. Oldenburg et al., "Nanoengineering of optical resonances," *Chem. Phys. Lett.* **288**, 243–247 (1998).
96. F. Kim et al., "Platonic gold nanocrystals," *Angew. Chem. Int. Ed.* **43**, 3673–3677 (2004).
97. A. K. Rengan et al., "Gold nanocages as effective photothermal transducers in killing highly tumorigenic cancer cells," *Part. Part. Syst. Char.* **31**, 398–405 (2014).
98. S. Wang et al., "Single continuous wave laser induced photodynamic/plasmonic photothermal therapy using photosensitizer-functionalized gold nanostars," *Adv. Mater.* **25**, 3055–3061 (2013).
99. X. C. Wang et al., "Understanding the photothermal effect of gold nanostars and nanorods for biomedical applications," *RSC Adv.* **4**, 30375–30383 (2014).
100. W. X. Niu et al., "Highly symmetric gold nanostars: crystallographic control and surface-enhanced raman scattering property," *J. Am. Chem. Soc.* **137**, 10460–10463 (2015).

101. Y. C. Wang et al., "Comparison study of gold nanohexapods, nanorods, and nanocages for photothermal cancer treatment," *ACS Nano* **7**, 2068–2077 (2013).
102. J. M. Luther et al., "Localized surface plasmon resonances arising from free carriers in doped quantum dots," *Nat. Mater.* **10**, 361–366 (2011).
103. J. W. Xiao et al., "Porous Pd nanoparticles with high photothermal conversion efficiency for efficient ablation of cancer cells," *Nanoscale* **6**, 4345–4351 (2014).
104. S. C. Boca et al., "Chitosan-coated triangular silver nanoparticles as a novel class of biocompatible, highly effective photothermal transducers for in vitro cancer cell therapy," *Cancer Lett.* **311**, 131–140 (2011).
105. H. K. Moon, S. H. Lee, and H. C. Choi, "In vivo near-infrared mediated tumor destruction by photothermal effect of carbon nanotubes," *ACS Nano* **3**, 3707–3713 (2009).
106. T. Mocan et al., "Photothermal treatment of human pancreatic cancer using PEGylated multi-walled carbon nanotubes induces apoptosis by triggering mitochondrial membrane depolarization mechanism," *J. Cancer* **5**, 679–688 (2014).
107. Z. Liu et al., "Carbon materials for drug delivery & cancer therapy," *Mater. Today* **14**(7–8), 316–323 (2011).
108. B. Tian et al., "Photothermally enhanced photodynamic therapy delivered by nano-graphene oxide," *ACS Nano* **5**, 7000–7009 (2011).
109. K. Yang et al., "Graphene in mice: ultrahigh in vivo tumor uptake and efficient photothermal therapy," *Nano Lett.* **10**, 3318–3323 (2010).
110. K. Yang et al., "Nano-graphene in biomedicine: theranostic applications," *Chem. Soc. Rev.* **42**, 530–547 (2013).
111. Y. Q. Yang et al., "Graphene based materials for biomedical applications," *Mater. Today* **16**(10), 365–373 (2013).
112. K. Leung, "Cypate-2-Deoxy-d-glucose," in *Molecular Imaging and Contrast Agent Database (MICAD)*, National Center for Biotechnology Information (US), Bethesda, Maryland (2004).
113. L. Wang et al., "Cypate-conjugated porous upconversion nanocomposites for programmed delivery of heat shock protein 70 small interfering RNA for gene silencing and photothermal ablation," *Adv. Funct. Mater.* **26**, 10–28 (2016).
114. C. Jin et al., "Ablation of hypoxic tumors with dose-equivalent photothermal, but not photodynamic, therapy using a nanostructured porphyrin assembly," *ACS Nano* **7**, 2541–2550 (2013).
115. K. A. Carter et al., "Porphyrin-phospholipid liposomes permeabilized by near-infrared light," *Nat. Commun.* **5**, 3546 (2014).
116. L. Yan and L. Y. Qiu, "Indocyanine green targeted micelles with improved stability for near-infrared image-guided photothermal tumor therapy," *Nanomedicine* **10**, 361–373 (2015).
117. M. B. Zheng et al., "Robust ICG theranostic nanoparticles for folate targeted cancer imaging and highly effective photothermal therapy," *ACS Appl. Mater. Interfaces* **6**, 6709–6716 (2014).
118. P. F. Zhao et al., "Improving drug accumulation and photothermal efficacy in tumor depending on size of ICG loaded lipid-polymer nanoparticles," *Biomaterials* **35**, 6037–6046 (2014).
119. A. M. Chang et al., "Alteration of heat shock protein 70 expression levels in term and preterm delivery," *J. Matern.-Fetal Neonat. Med.* **26**, 1581–1585 (2013).
120. Y. Ma et al., "Indocyanine green loaded SPIO nanoparticles with phospholipid-PEG coating for dual-modal imaging and photothermal therapy," *Biomaterials* **34**, 7706–7714 (2013).
121. L. Wu et al., "Hybrid polypeptide micelles loading indocyanine green for tumor imaging and photothermal effect study," *Biomacromolecules* **14**, 3027–3033 (2013).
122. J. Yu et al., "Self-assembly synthesis, tumor cell targeting, and photothermal capabilities of antibody-coated indocyanine green nanocapsules," *J. Am. Chem. Soc.* **132**, 1929–1938 (2010).
123. H. M. Subhash et al., "Optical detection of indocyanine green encapsulated biocompatible poly (lactic-co-glycolic) acid nanoparticles with photothermal optical coherence tomography," *Opt. Lett.* **37**, 981–983 (2012).
124. C. D. Geddes, H. Cao, and J. R. Lakowicz, "Enhanced photostability of ICG in close proximity to gold colloids," *Spectrochim. Acta Part A* **59**, 2611–2617 (2003).
125. S. Gupta et al., "Indocyanine green clearance test (using spectrophotometry) and its correlation with model for end stage liver disease (MELD) score in Indian patients with cirrhosis of liver," *Trop. Gastroenterol.* **33**, 129–134 (2012).
126. X. L. Liang et al., "PEGylated polypyrrole nanoparticles conjugating gadolinium chelates for dual-modal MRI/photoacoustic imaging guided photothermal therapy of cancer," *Adv. Funct. Mater.* **25**, 1451–1462 (2015).
127. X. J. Song et al., "Photosensitizer-conjugated albumin-polypyrrole nanoparticles for imaging-guided in vivo photodynamic/photothermal therapy," *Small* **11**, 3932–3941 (2015).
128. R. P. Zhang et al., "Engineering melanin nanoparticles as an efficient drug-delivery system for imaging-guided chemotherapy," *Adv. Mater.* **27**, 5063–5069 (2015).
129. Y. Liu et al., "Dopamine-melanin colloidal nanospheres: an efficient near-infrared photothermal therapeutic agent for in vivo cancer therapy," *Adv. Mater.* **25**, 1353–1359 (2013).
130. D. Wang, M. T. Carlson, and H. H. Richardson, "Absorption cross section and interfacial thermal conductance from an individual optically excited single-walled carbon nanotube," *ACS Nano* **5**, 7391–7396 (2011).
131. B. del Rosal et al., "Neodymium-based stoichiometric ultrasmall nanoparticles for multifunctional deep-tissue photothermal therapy," *Adv. Opt. Mater.* **4**, 782–789 (2016).
132. Y. Liu et al., "Understanding the toxicity of carbon nanotubes," *Acc. Chem. Res.* **46**, 702–713 (2013).
133. H. S. Choi et al., "Renal clearance of quantum dots," *Nat. Biotechnol.* **25**, 1165–1170 (2007).
134. E. B. Ehlerding, F. Chen, and W. B. Cai, "Biodegradable and renal clearable inorganic nanoparticles," *Adv. Sci.* **3**, 1500223 (2016).
135. J. B. Liu et al., "Passive tumor targeting of renal-clearable luminescent gold nanoparticles: long tumor retention and fast normal tissue clearance," *J. Am. Chem. Soc.* **135**, 4978–4981 (2013).
136. C. Alric et al., "The biodistribution of gold nanoparticles designed for renal clearance," *Nanoscale* **5**, 5930–5939 (2013).
137. G. Sonavane, K. Tomoda, and K. Makino, "Biodistribution of colloidal gold nanoparticles after intravenous administration: effect of particle size," *Colloid Surf. B* **66**, 274–280 (2008).
138. M. A. Mackey et al., "The most effective gold nanorod size for plasmonic photothermal therapy: theory and in vitro experiments," *J. Phys. Chem. B* **118**, 1319–1326 (2014).
139. E. E. Connor et al., "Gold nanoparticles are taken up by human cells but do not cause acute cytotoxicity," *Small* **1**, 325–327 (2005).
140. K. C. L. Black et al., "Radioactive Au-198-doped nanostructures with different shapes for in vivo analyses of their biodistribution, tumor uptake, and intratumoral distribution," *ACS Nano* **8**, 4385–4394 (2014).
141. A. M. Goodman et al., "The surprising in vivo instability of near-IR-absorbing hollow Au-Ag nanoshells," *ACS Nano* **8**, 3222–3231 (2014).
142. L. Cavigli et al., "Size affects the stability of the photoacoustic conversion of gold nanorods," *J. Phys. Chem. C* **118**, 16140–16146 (2014).
143. S. Jain, D. G. Hirst, and J. M. O'sullivan, "Gold nanoparticles as novel agents for cancer therapy," *Br. J. Radiol.* **85**, 101–113 (2012).
144. S. T. Yang et al., "Long-term accumulation and low toxicity of single-walled carbon nanotubes in intravenously exposed mice," *Toxicol. Lett.* **181**, 182–189 (2008).
145. M. Adeli et al., "Carbon nanotubes in cancer therapy: a more precise look at the role of carbon nanotube-polymer interactions," *Chem. Soc. Rev.* **42**, 5231–5256 (2013).
146. D. P. K. Lankveld et al., "Blood clearance and tissue distribution of PEGylated and non-PEGylated gold nanorods after intravenous administration in rats," *Nanomedicine* **6**, 339–349 (2011).
147. A. R. Lowery et al., "Immunonanoshells for targeted photothermal ablation of tumor cells," *Int. J. Nanomed.* **1**, 149–154 (2006).
148. A. Baliaka et al., "Intratumoral gene therapy versus intravenous gene therapy for distant metastasis control with 2-diethylaminoethyl-dextran methyl methacrylate copolymer non-viral vector-p53," *Gene Ther.* **21**, 158–167 (2014).
149. X. Zheng et al., "Enhanced tumor treatment using biofunctional indocyanine green-containing nanostructure by intratumoral or intravenous injection," *Mol. Pharm.* **9**, 514–522 (2012).

150. J. Beik et al., "Nanotechnology in hyperthermia cancer therapy: from fundamental principles to advanced applications," *J. Control Release* **235**, 205–221 (2016).
151. F. Danhier, O. Feron, and V. Preat, "To exploit the tumor microenvironment: passive and active tumor targeting of nanocarriers for anti-cancer drug delivery," *J. Control Release* **148**, 135–146 (2010).
152. H. Y. Karasulu, B. Karaca, and E. Karasulu, "Classification and application of colloidal drug delivery systems passive or active tumor targeting," *Surfactant Sci. Ser.* **148**, 545–561 (2010).
153. Y. H. Bae and K. Park, "Targeted drug delivery to tumors: myths, reality and possibility," *J. Control Release* **153**, 198–205 (2011).
154. I. H. El-Sayed, X. H. Huang, and M. A. El-Sayed, "Selective laser photo-thermal therapy of epithelial carcinoma using anti-EGFR antibody conjugated gold nanoparticles," *Cancer Lett.* **239**, 129–135 (2006).
155. A. R. Lowery et al., "Immunonanoshells for selective photothermal therapy," *Clin. Cancer Res.* **11**, 9097s–9097s (2005).
156. J. Fang and Y. C. Chen, "Nanomaterials for photohyperthermia: a review," *Curr. Pharm. Des.* **19**, 6622–6634 (2013).
157. J. Chen et al., "Au–silica nanowire nanohybrid as a hyperthermia agent for photothermal therapy in the near-infrared region," *Langmuir* **30**, 9514–9523 (2014).
158. B. K. Jung et al., "Mild hyperthermia induced by gold nanorod-mediated plasmonic photothermal therapy enhances transduction and replication of oncolytic adenoviral gene delivery," *ACS Nano* **10**, 10533–10543 (2016).
159. W. Jiang et al., "Remodeling tumor vasculature to enhance delivery of intermediate-sized nanoparticles," *ACS Nano* **9**, 8689–8696 (2015).
160. B. V. Harmon et al., "The role of apoptosis in the response of cells and tumours to mild hyperthermia," *Int. J. Radiat. Biol.* **59**, 489–501 (1991).
161. R. K. Jain and T. Stylianopoulos, "Delivering nanomedicine to solid tumors," *Nat. Rev. Clin. Oncol.* **7**, 653–664 (2010).
162. K. J. Fuller et al., "Cancer and the heat shock response," *Eur. J. Cancer* **30A**, 1884–1891 (1994).
163. J. T. Kovalchin et al., "In vivo delivery of heat shock protein 70 accelerates wound healing by up-regulating macrophage-mediated phagocytosis," *Wound Repair Regener.* **14**, 129–137 (2006).
164. D. R. Ciocca and S. K. Calderwood, "Heat shock proteins in cancer: diagnostic, prognostic, predictive, and treatment implications," *Cell Stress Chaperones* **10**, 86–103 (2005).
165. B. K. Wang et al., "Gold-nanorods-siRNA nanoplex for improved photothermal therapy by gene silencing," *Biomaterials* **78**, 27–39 (2016).
166. A. Lopez-Noriega et al., "Thermally triggered release of a pro-osteogenic peptide from a functionalized collagen-based scaffold using thermosensitive liposomes," *J. Control Release* **187**, 158–166 (2014).
167. C. M. J. Hu et al., "Erythrocyte membrane-camouflaged polymeric nanoparticles as a biomimetic delivery platform," *Proc. Natl. Acad. Sci. U. S. A.* **108**, 10980–10985 (2011).
168. W. Zhang et al., "Synergistic effect of chemo-photothermal therapy using PEGylated graphene oxide," *Biomaterials* **32**, 8555–8561 (2011).
169. M. Zheng et al., "Single-step assembly of DOX/ICG loaded lipid—polymer nanoparticles for highly effective chemo-photothermal combination therapy," *ACS Nano* **7**, 2056–2067 (2013).
170. Y. D. Jin, "Multifunctional compact hybrid Au nanoshells: a new generation of nanoplasmonic probes for biosensing, imaging, and controlled release," *Acc. Chem. Res.* **47**, 138–148 (2014).
171. J. Kim et al., "Designed fabrication of multifunctional magnetic gold nanoshells and their application to magnetic resonance imaging and photothermal therapy," *Angew. Chem. Int. Ed.* **45**, 7754–7758 (2006).
172. L. Gu, A. R. Koymen, and S. K. Mohanty, "Crystalline magnetic carbon nanoparticle assisted photothermal delivery into cells using CW near-infrared laser beam," *Sci. Rep.* **4**, 5106 (2014).
173. G. V. Orsinger, J. D. Williams, and M. Romanowski, "Focal activation of cells by plasmon resonance assisted optical injection of signaling molecules," *ACS Nano* **8**, 6151–6162 (2014).
174. S. P. Sherlock et al., "Photothermally enhanced drug delivery by ultrasmall multifunctional FeCo/graphitic shell nanocrystals," *ACS Nano* **5**, 1505–1512 (2011).
175. E. Y. Lukianova-Hleb et al., "On-demand intracellular amplification of chemoradiation with cancer-specific plasmonic nanobubbles," *Nat. Med.* **20**, 778–784 (2014).
176. H. Hosoya et al., "Integrated nanotechnology platform for tumor-targeted multimodal imaging and therapeutic cargo release," *Proc. Natl. Acad. Sci. U. S. A.* **113**, 1877–1882 (2016).
177. D. Wu et al., "GJIC Enhances the phototoxicity of photofrin-mediated photodynamic treatment by the mechanisms related with ROS and calcium pathways," *J. Biophotonics* **8**, 764–774 (2015).
178. M. H. Xu and L. H. V. Wang, "Photoacoustic imaging in biomedicine," *Rev. Sci. Instrum.* **77**, 041101 (2006).
179. L. Z. Xiang et al., "Gold nanoshell-based photoacoustic imaging application in biomedicine," in *Proc. of Int. Symp. on Biophotonics, Nanophotonics and Metamaterials*, pp. 72–75 (2006).
180. P. Huang et al., "Biodegradable gold nanovesicles with an ultrastrong plasmonic coupling effect for photoacoustic imaging and photothermal therapy," *Angew. Chem. Int. Ed.* **52**, 13958–13964 (2013).
181. Y. Yong et al., "Tungsten sulfide quantum dots as multifunctional nanotheranostics for in vivo dual-modal image-guided photothermal/radiotherapy synergistic therapy," *ACS Nano* **9**, 12451–12463 (2015).
182. X. R. Song et al., "Co_9Se_8 nanoplates as a new theranostic platform for photoacoustic/magnetic resonance dual-modal-imaging-guided chemo-photothermal combination therapy," *Adv. Mater.* **27**, 3285–3291 (2015).
183. W. Y. Yin et al., "High-throughput synthesis of single-layer MoS_2 nanosheets as a near-infrared photothermal-triggered drug delivery for effective cancer therapy," *ACS Nano* **8**, 6922–6933 (2014).
184. B. Li et al., "$Cu_{7.2}S_4$ nanocrystals: a novel photothermal agent with a 56.7% photothermal conversion efficiency for photothermal therapy of cancer cells," *Nanoscale* **6**, 3274–3282 (2014).
185. T. Liu et al., "Drug delivery with PEGylated MoS_2 nano-sheets for combined photothermal and chemotherapy of cancer," *Adv. Mater.* **26**, 3433–3440 (2014).
186. S. H. Wang et al., "Plasmonic copper sulfide nanocrystals exhibiting near-infrared photothermal and photodynamic therapeutic effects," *ACS Nano* **9**, 1788–1800 (2015).
187. J. H. Appel et al., "Low cytotoxicity and genotoxicity of two-dimensional MoS_2 and WS_2," *ACS Biomater. Sci. Eng.* **2**, 361–367 (2016).
188. K. Yang et al., "Multimodal imaging guided photothermal therapy using functionalized graphene nanosheets anchored with magnetic nanoparticles," *Adv. Mater.* **24**, 1868–1872 (2012).
189. W. R. Chen et al., "Chromophore-enhanced laser-tumor tissue photothermal interaction using an 808-nm diode-laser," *Cancer Lett.* **88**, 15–19 (1995).
190. W. R. Chen et al., "Photothermal effects on murine mammary tumors using indocyanine green and an 808-nm diode laser: an in vivo efficacy study," *Cancer Lett.* **98**, 169–173 (1996).
191. B. M. Barth et al., "Targeted indocyanine-green-loaded calcium phosphosilicate nanoparticles for in vivo photodynamic therapy of leukemia," *ACS Nano* **5**, 5325–5337 (2011).
192. S. M. El-Daly et al., "Photodynamic therapeutic activity of indocyanine green entrapped in polymeric nanoparticles," *Photodiagn. Photodyn. Ther.* **10**, 173–185 (2013).

Wangzhong Sheng received his BS degree in materials science engineer from Cornell University and is currently pursuing his PhD at the University of California San Diego with Prof. Adah Almutairi. For his thesis work, he developed a technique involving gold-nanoparticle laser-assisted photothermal pretreatment of adipose tissue to aid liposuction, called NanoLipo, and is currently pursuing its clinical translation. He is also well-trained in formulations chemistry and methods for encapsulating small molecules drugs in various drug-delivery vehicles.

Sha He received his BS degree in biomedical engineering from Huazhong University of Science and Technology in 2009, MS degree in biomedical engineering from Chongqing University in 2012 under the joint guidance of Prof. Xingyu Jiang and Prof. Kaiyong Cai, and is now a PhD candidate in nanoengineering at the University of California San Diego with Prof. Adah Almutairi. His current research interests include doping and epitaxy of colloidal lanthanide nanoparticles and their optical applications.

William J. Seare received his medical degree from the University of Utah, College of Medicine, where he also completed two residencies. He is a doubly board certified orthopedic and plastic surgeon practicing in Carlsbad, California, USA, using only awake anesthesia. He performs aggressive, large volume liposuction in combination Avelar abdominoplasties and fat transfer to the buttocks, breasts, and face. He uses clinical and research methods to improve body contouring procedures at his clinic.

Adah Almutairi is a faculty member at the University of California San Diego with her primary appointment in the Skaggs School of Pharmacy and Pharmaceutical Sciences. She is also the codirector of UCSD's Center of Excellence in Nanomedicine, a rapidly expanding interdisciplinary research collaborative team developing tools for the future of biology and medicine. She came to UCSD from UC Berkeley, where she worked with Prof. Jean Fréchet to develop several nanoprobes for *in vivo* imaging.